Mechanical Systems and Signal Processing 104 (2018) 494–502

Contents lists available at ScienceDirect

Mechanical Systems and Signal Processing

journal homepage: www.elsevier.com/locate/ymssp

Predicting catastrophes of non-autonomous networks with visibility graphs and horizontal visibility

Haicheng Zhang [a], Daolin Xu [a,*], Yousheng Wu [b]

[a] State Key Laboratory of Advanced Design and Manufacturing for Vehicle Body, Hunan University, Changsha 410082, PR China
[b] China Ship Scientific Research Center, Wuxi 214082, PR China

ARTICLE INFO

Article history:
Received 15 August 2017
Received in revised form 20 October 2017
Accepted 14 November 2017

Keywords:
Catastrophes
Pre-warning
Complex network
Visibility graphs

ABSTRACT

Prediction of potential catastrophes in engineering systems is a challenging problem. We first attempt to construct a complex network to predict catastrophes of a multi-modular floating system in advance of their occurrences. Response time series of the system can be mapped into an virtual network by using visibility graph or horizontal visibility algorithm. The topology characteristics of the networks can be used to forecast catastrophes of the system. Numerical results show that there is an obvious corresponding relationship between the variation of topology characteristics and the onset of catastrophes. A Catastrophe Index (CI) is proposed as a numerical indicator to measure a qualitative change from a stable state to a catastrophic state. The two approaches, the visibility graph and horizontal visibility algorithms, are compared by using the index in the reliability analysis with different data lengths and sampling frequencies. The technique of virtual network method is potentially extendable to catastrophe predictions of other engineering systems.

1. Introduction

Catastrophic events happen occasionally in various fields such as economic system, ecology system, biology system and engineering system [1–4]. Especially, modern systems rarely isolated and inextricably interlinked in complex manners [5,6], and mutual interaction among sub-systems will increased systemic risks [7,8] and lead to cascading catastrophes [9]. A question of paramount importance is how to predict catastrophes in advance of their possible occurrences to avoid heavy casualties and serious economic losses [10].

Catastrophic events can occur in different forms among which bifurcation cascades, sudden change, crisis, etc., caused by nonlinear properties are universal in engineering system [11]. There are abundant research works about predicting the onset of catastrophes using bifurcation or catastrophic theory [12] based on the established complete mathematical model. The above method relies on prerequisites that the underlying system is completely known. However, there is no exaggeration to say that most systems are unavailable for precise mathematical models due to the complexity in the real world. Prediction of potential catastrophes without models of underlying dynamical system becomes especially challenging. There are various efforts to predict dynamical systems via reconstructing systems based on time series using nonlinear dynamic theory [13]. The scope of these methods ranges from phase space methods [14,15] to time delay embedding methods [16]. However,

* Corresponding author.
E-mail addresses: zhanghc@hnu.edu.cn (H. Zhang), dlxu@hnu.edu.cn (D. Xu), wuys@cssrc.com.cn (Y. Wu).

https://doi.org/10.1016/j.ymssp.2017.11.020
0888-3270/

quickly and reliably predicting is still an issue due to the local reconstruction and the difficulty with the required computations [10].

Complex network theory has undergone a remarkable development in the last decades [17–19], which provide us a new insight to deal with complex systems from different disciplines [20–24]. Very recently, a pioneer work [25] has greatly promoted the work in time series analysis, where Zhang and Small first proposed a mapping method to convert time series to complex networks to analyze pseudo-periodic time series. Different from the above method in which the virtual networks were mapped from the reconstructed phase space or the linear correlation coefficient, Lacasa et al. proposed a quite simple mapping method, named visibility graph (VG) [26] and subsequent horizontal visibility graph (HVG) [27], which can inherit the time series properties in the structure of the associated graphs. Owing to the advantages, such as low computational cost, straightforward implementation and easy way to find connections, the method becomes popular and applicable in various fields [28]. Flanagan and Lacasa made use of visibility algorithms to quantify the irreversibility of the financial time series [29]. Liu et al. studied the statistical properties of complex networks constructed from time series of energy dissipation rates in three-dimensional fully developed turbulence using the visibility algorithm [30]. Elsner et al. demonstrated how to construct a network from a time series of U.S. hurricane counts and showed how it can be used to identify unusual years in the record [31]. Luque et al. provided a complete graph theoretical characterization of iterated maps undergoing period doubling route to chaos based on HVG algorithm [32]. Li and Dong constructed networks of human ventricular time series with the visibility graph approach to detect and predict the onset of human ventricular fibrillation [33]. Apart from applications listed above, there are abundant related research works documented in the review literature [28]. However, both the mathematical grounding of this promising theory and its applications are in its infancy [34].

In this paper, we first attempt to introduce the complex network method to predict potential catastrophes of non-autonomous network systems. The model of the multi-modular floating structure is selected from [35] for the case studies because this system is typical and complicated enough in the representation of a wide range of non-autonomous multi-body systems in engineering field. The pre-warning of catastrophes from transient dynamics of such dynamic systems is important for the concerns of engineering safety. However this important topic still remains untouched especially for multi-modular floating systems in the field of offshore engineering. The non-autonomous system can exhibit the interesting phenomenon of amplitude death (AD), a state that all oscillators in the network are mutually confined in a very weak oscillatory state [36]. The system may also undergo a sudden change from amplitude death state to a large oscillation state at certain critical parameters which can threaten or even destroy the system. The sudden change in dynamics is here regarded as a catastrophe that one strives to avoid at all cost. We translate dynamical properties of time series into structural features of graphs via mapping response time series to graphic network based on VG and HVG algorithms. By studying the average degree of the VG graph and the maximum degree of the HVG graph, the onset of catastrophes can be predicted in advance of their occurrences. We further propose a numerical indicator, named as Catastrophe Index (CI), to measure a qualitative change from a stable state to a catastrophic state. The performance of the two approaches, visibility graph and horizontal visibility, is compared by using the index in terms of the reliability with different data lengths and sampling frequencies. Numerical experiment is carried out for catastrophe identifications and verifies the feasibility and efficiency of this proposed method. The technique of using graphic networks to predict potential catastrophes is new and is not restricted to the case study of the floating system, but also in principle applicable to fault detection and diagnosis of mechanical systems.

2. Graphic networks for catastrophe prediction

Based on the modeling method [35], the model of a chained multi-module floating airport can be formed by integrating the dynamic model of a single floating module and coupling model of connector and the constraint model of the mooring system. The governing equation for an N-module floating structure can be generally written as

$$(\mathbf{M}_i + \boldsymbol{\mu}_i)\ddot{\mathbf{X}}_i + \boldsymbol{\lambda}_i\dot{\mathbf{X}}_i + (\mathbf{S}_i + \delta(i,i_0)\mathbf{K}_i)\mathbf{X}_i = \mathbf{F}^w e^{i(\omega t+\varphi_i)} + \varepsilon\sum_{j=1}^{N}\Phi_{ij}G(\mathbf{X}_i,\mathbf{X}_j), \quad i = 1,\cdots,N \tag{1}$$

where the symbol $\mathbf{X}_i = [x_i, z_i, \beta_i]^T$ denotes the displacement vector of the i-th module where the state variables x_i, z_i, β_i denote surge, heave and pitch motions respectively. $\mathbf{M}_i, \mathbf{S}_i$ indicate the mass matrix and the hydrostatic restoring coefficient matrix, respectively. The matrix $\mathbf{K}_i$ denotes the environmental constraint on the floating system that is moored by the catenaries in order to restrict the drifting, and $\delta(i,i_0)$ is the Delta function which determinates the position where the catenaries are installed. $\boldsymbol{\mu}_i, \boldsymbol{\lambda}_i$ and $\mathbf{F}^w$ represent the added mass, damping matrixes and exciting force vector respectively as a result of water waves. $\omega = 2\pi/T$ denotes the circular frequency of linear wave and T is wave period. φ_i denotes the initial phase angle of the i-th module due to a head wave propagating along the huge size of the floating airport and the phase delay is defined as $\Delta\varphi_{i(i+1)} = \varphi_{i+1} - \varphi_{i+1} = k(L_i + L_{i+1})/2$ of which k indicates wave number. The second term $\varepsilon\sum_{j=1}^{N}\Phi_{ij}G(\mathbf{X}_i,\mathbf{X}_j)$ on the right hand side of Eq. (1) denotes the coupling term which represents the mechanical features of the connection between the modules. The parameter ε indicates the coupling strength (stiffness of the connector). Φ is the coupling topology matrix, of which the element Φ_{ij} is set to 1 when the i-th module connects with j-th module otherwise Φ_{ij} is set to zero. $G(\mathbf{X}_i,\mathbf{X}_j)$ denotes the coupling function which describes the geometric relationship of the connection.

It is worth noting that the governing Eq. (1) is a generalized model for multi-module floating structure, which can deal with arbitrary topological configurations and connections with introducing the coupling topology matrix. In addition, due to the huge scale of the floating module, the displacements at the connection joints are usually large even if the pitch angles of the modules are small. Thus the model of the connector presents strong geometrical nonlinearity which may causes catastrophic event in certain wave conditions. Pre-warning of a catastrophic event has always been an important topic because it carries many passengers, crews and facilities.

In this paper, a virtual network method is proposed to predict potential catastrophes of the non-autonomous multi-body systems. A time series can be converted into an artificial network where the dynamic features of the time series are transferred to topology characteristics of the artificial network. The VG [26] and HVG [27] algorithms suggested by Lacasa et al. will be employed to implement the conversion and further prediction method of catastrophes is developed. Based on the algorithms, each data point of time series is mapped to form nodes of the artificial network. The node whether or not connecting with other nodes depends on the visibility criterion: two arbitrary nodes $x(t_i)$ and $x(t_j)$ mapped from a time series become two connected nodes in an associated graph, if any other data $(t_k, x(t_k))$ placed between them $(t_i < t_k < t_j)$ fulfills, for VG algorithm shown in Fig. 1(a),

$$\frac{x(t_j)-x(t_i)}{t_j-t_i} > \frac{x(t_k)-x(t_i)}{t_k-t_i}, \qquad \forall t_k \in [t_i, t_j] \tag{2}$$

and for HVG algorithm shown in Fig. 1(b),

$$x(t_j), x(t_i) > x(t_k), \qquad \forall t_k \in [t_i, t_j] \tag{3}$$

According to above mapping methods, the dynamic characteristics of a time series can be represented by the topology characteristics of the corresponding network graph. The topology structure of an undirected and unweighted complex network can be described by the adjacent matrix A where its element is assigned as $A_{ij} = 1$, if the node i is connected with node j and otherwise $A_{ij} = 0$. The node degree, a simple but important property, is to be used to predict catastrophes. The node degree k_i of a node i is defined as the number of connections of node i. Hence, the degree of a node is the number of edges that it shares with other nodes [37], defined as

$$k_i = \sum_{j=1}^{N_s} A_{ij} = \sum_{j=1}^{N_s} A_{ji} \tag{4}$$

and the average node degree of a network is the average of k_i for all nodes in the network

$$\langle k \rangle = \frac{1}{N_s}\sum_{j=1}^{N_s} k_i = \frac{1}{N_s}\sum_{i=1}^{N_s}\sum_{j=1}^{N_s} A_{ij} \tag{5}$$

In this paper, the average node degree of VG and the maximum node degree of HVG is used in later analysis considering the insensitivity of the average node degree of HVG which is in the interval of $2 \leqslant \langle k \rangle \leqslant 4$ [34]. Different from the average node degree calculated from the whole range of time series, the local property, maximum node degree, is used for the HVG,

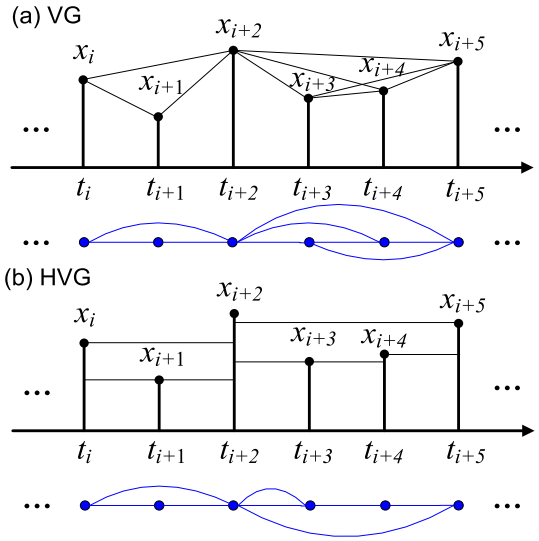

Fig. 1. Illustration of mapping a time series $\{x_i\}$ to network graph with (a) visibility graph algorithm and (b) horizontal visibility graph algorithm.

which is more impressionable to noise than the average node degree of HVG is. Thus a modified HVG algorithm, namely filtered Horizontal Visibility Graph (f-HVG), is used to avoid the influence of noise and the visibility criterion (3) will be modified as [34]

$$x(t_j), x(t_i) > x(t_k) + \bar{f}, \qquad \forall t_k \in [t_i, t_j] \tag{6}$$

where $\bar{f}$ is a filter defined as a real valued scalar, which is determined by the Signal to Noise Ratio (SNR) of the observed time series.

3. Numerical Illustration

In this paper, a floating airport, consisting of five identical box type floating modules serially connected by the parallel hinge connectors, is considered as the case study for numerical simulations. As the main purpose of this work is to illustrate the feasibility of the complex network reconstruction for catastrophe prediction of the floating airport, we referred to the same parameterization as in [35] basically to avoid tedious and repeating explanation of structure configuration and related parameters, which may blur the focus of this paper on the network prediction method. Without loss of generality, the non-dimensional response amplitude of the modules, named as response amplitude operator (RAO) for the marine structure, and non-dimensional coupling strength are introduced for the two dimensional system, written as

$$z^* = z/a, \qquad \varepsilon^* = (\varepsilon T^2)/(\rho h^2 \cdot 1) \tag{7}$$

where the symbols a, ρ, h denote wave amplitude, water density and water depth respectively. In order to write easily, we use the symbols without asterisk in superscript to represent the non-dimensional parameters in the following context.

We first illustrate the dynamic behaviors of this floating system to understand its catastrophic features. Fig. 2(a) shows the RAO of heave motion versus non-dimensional coupling strength ε. From Fig. 2(a) we can see that the amplitudes of all oscillators remain at a lower level, regarded as the amplitude death (AD) [36], in the three intervals of the parameter $0 < \varepsilon < 2.44, 4.02 < \varepsilon < 5.32, \varepsilon > 7.42$ and the response amplitudes may be simultaneously and significantly amplified in a rapid fashion at critical values, regarded as jumps. The mechanism of amplitude death is that there exist several solution branches for the nonlinear system and amplitude death happens when the steady state of the system falls into a weak oscillation solution branch [38]. A jump phenomenon terminates the AD state, which is regarded as an onset of catastrophe for the marine system. In order to understand the catastrophe features, we scrutinize the oscillation patterns by the bifurcation diagram, shown in Fig. 2(b). The response corresponding to an AD state is a harmonic motion of which the oscillation period coincides with the excitation period exactly. In our tremendous numerical studies of the multi-modular systems, either two dimensional floating airport coupled by rubber-cable connectors [39] or the three dimensional floating airport connected with elastic hinged connectors [40], all revealed the similar feature that the time series of system responses usually accompany with the faint high-order harmonic components before a catastrophe event comes. The faint components of high-order harmonics could be unsteady, so that the frequency domain analysis works no void. The proposed network method enables to identify qualitative changes of time series with high-order harmonics.

Assume that we do not know the mathematical model of the floating system for a real engineering system. We want to predict catastrophic events based on the time series of system responses. Although there are flexible choices of using a number of time series collected from motions of different modules and different degrees of freedom, here we only use a time series of heave motion of the third module, which is sufficient for the usage of catastrophic prediction due to the network synergistic effect [41].

To better illustrate our method, without loss of generality, we introduce two non-dimensional parameters, data length $N_T = (t_{N_s} - t_0)/T$ and sampling frequency $f = f_s/f_0$ where f_s is the actual sampling frequency and $f_0 = 1/T$ denotes the

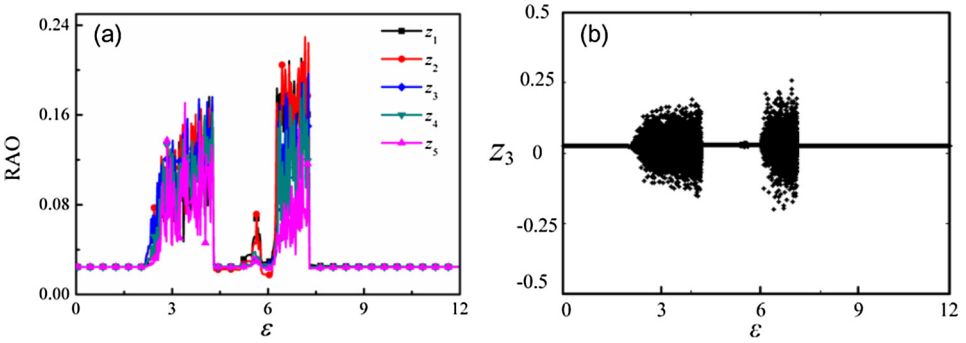

Fig. 2. Variation of dynamic response of a non-autonomous network in a parameter range; (a) the response amplitude operator of heave motion in different modules, (b) the stroboscopic bifurcation diagram of the heave response z_3 of the third module as the coupling strength ε sweeps forwards with the parameter settings of $T = 10$ s, $N = 5$.

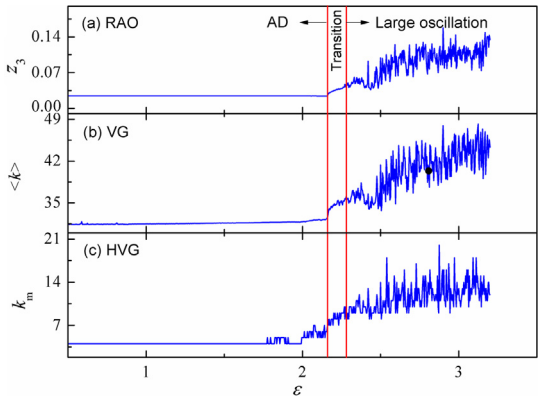

Fig. 3. Variation of dynamic response and corresponding topology characteristics of network graphs generated through the visibility algorithm and the horizontal visibility algorithm for time series for sampling frequency $f = 50$ and data length $N_T = 50$; (a) the response amplitude operator of the state variable z_3, (b) average node degree of visibility graph and (c) maximum node degree of horizontal visibility graph.

excitation frequency. Fig. 3(a) illustrates the response amplitude operator of the state variable z_3 in the partial interval of coupling strength in Fig. 2(a) with the filter $\bar{f} = 1 \times 10^{-4}$. Fig. 3(b) and (c) illustrate the average node degree of the VG and the maximum node degree of the HVG mapped from corresponding time series. From Fig. 3(a) we can see that there is a transition region between the region of AD and large oscillation state. In this region, response amplitude increases and the sub-harmonic motion appears when its time series is examined in frequency spectrum. From Fig. 3(b) and (c), we can see that the changes of average node degree of the VG and the maximum node degree of the HVG have the similar trends as shown in Fig. 3(a). When the response evolves from an AD state to large oscillation state, namely the occurrence of catastrophe, the corresponding average node degree and maximum node degree of the networks will increase. This congruent relationship between the response time series and the topology characteristics of the networks can be used to predict the occurrence of catastrophe. In order to further confirm the reliability of the corresponding relationship, we choose three typical cases in the three parameter regions picked at $\varepsilon = 1.2, \varepsilon = 2.2, \varepsilon = 2.8$ for different motion patterns, to show the dynamic variations and the corresponding networks, shown in Fig. 4.

Fig. 4 illustrates three examples of the artificial networks constructed from time series of different motion patterns. From the left to right column, the time series correspond to an AD state (single period motion), a transition state (multi-harmonic motion) and large oscillation state (chaotic motion), and the networks are formed by the VG algorithm (second row) and the HVG algorithm (third row), drawn by the Gephi software [42]. From the three corresponding networks for VG algorithm, we can see that the network becomes more and more dense with the increase of coupling strength and the average node degree of the three networks is $\langle k \rangle = 31.537, 34.493, 38.410$ respectively. When we observe the network graph carefully, we find that there are different numbers of the graph hubs for the three networks and the numbers of the hubs corresponds to the numbers of the dominant response amplitudes. The first network for $\varepsilon = 1.2$ has 50 graph hubs due to the data length $N_T = 50$, the second network for $\varepsilon = 2.2$ has four hubs which corresponds to the four response peaks and there is one dominant hubs for the third network for $\varepsilon = 2.8$ due to the chaotic motion. The average node degree of the three networks for HVG is $\langle k \rangle = 3.783, 3.849, 3.856$ respectively. Different from the networks for VG algorithm, the density of the networks for HVG algorithm has insignificant change for different coupling strengths in comparison with the second row and the third row of Fig. 4, while in contrast the maximum node degree of the network is $k_m = 4, 9, 11$ respectively. This is the reason why we use the maximum degree instead of the average degree of the HVG graph to predict catastrophes. In fact, the previous work revealed that the node with the maximum node degree, namely the most connected node, are the data with largest response values, which corresponds to the extreme events of the series [27].

In order to evaluate the performance of the proposed method, we propose Catastrophe Index (CI) as a numerical indicator to quantify a qualitative change from a stable state to a catastrophic state. The index CI is designed as follows. First, determine a benchmark state of the topological characteristic μ_0 (either average node degree or maximum node degree) of the network from a stable state of an original system. Then, devise a transient characteristic μ that is the instant topological characteristic of the network from the present evolutionary state of the system. Therefore, the time-dependent index C_μ is introduced to define the rate of qualitative change of responses, given by

$$C_\mu = \frac{\mu - \mu_0}{\mu_0} \times 100\% \tag{8}$$

From the above definition of the index C_μ, we know that if the floating system is in a stable state, the transient topology characteristic μ is close to the benchmark value μ_0 and the index C_μ tends to be zero; If the floating system is about the occurrence of a catastrophic event, the time series usually accompanies with the emergence of sub-harmonic or aperiodic components in the observed time series, resulting that μ deviates from μ_0 and the index C_μ diverges from zero. Variation of the index signifies an oncoming disaster event.

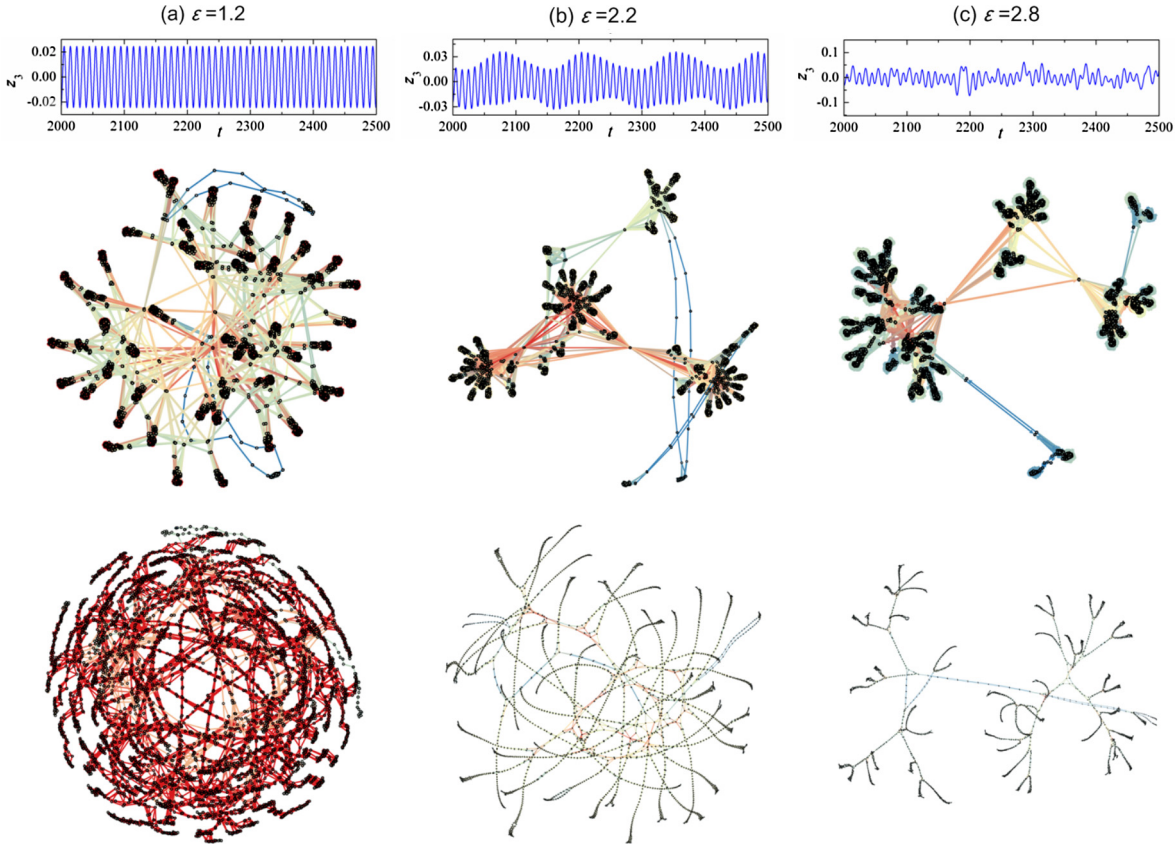

Fig. 4. Time series (the first row) and corresponding network graphs constructed by the visibility algorithm (the second row) and the horizontal visibility algorithm (the third row), for different coupling strengths (a) $\varepsilon = 1.2$, (b) $\varepsilon = 2.2$, and (c) $\varepsilon = 2.8$.

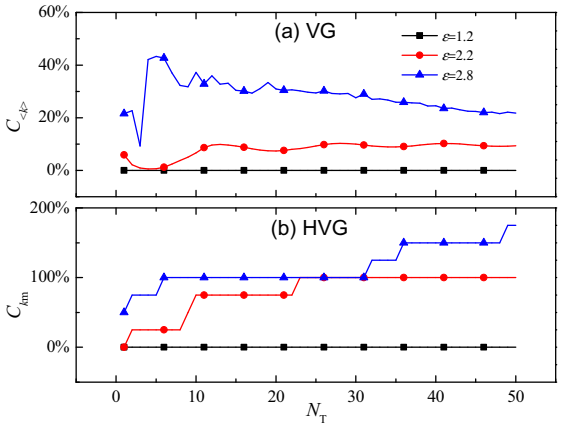

Fig. 5. (a) The CI for the average node degree of the visibility graph and (b) the CI for the maximum node degree of the horizontal visibility graph, as a function of data length for the sampling frequency $f = 50$.

In what follows, the two algorithms (VG and HVG) will be compared using CI in terms of the reliability with different data lengths and sampling frequencies. Fig. 5 illustrates the CI for the average node degree of the VG method and the CI for the maximum node degree of the HVG method under the change of data length N_T with sampling frequency $f = 50$ where the coupling strengths are picked at $\varepsilon = 1.2, \varepsilon = 2.2, \varepsilon = 2.8$ for different motion patterns. From Fig. 5(a) we can see that CI for the average node degree of the VG graph for stable state with coupling strength at $\varepsilon = 1.2$ always stays at zero. The CI for the average node degree with the coupling strengths at $\varepsilon = 2.2$ and $\varepsilon = 2.8$ have large fluctuation for small data length $N_T < 20$,

then CI for the coupling strength $\varepsilon = 2.2$ in the transition state reaches to a relative stable value around $C_{\langle k\rangle} = 10\%$ accompanied with weak fluctuation while CI for the coupling strength $\varepsilon = 2.8$ decreases weakly towards $C_{\langle k\rangle} = 20\%$ with the increase of data length. For the index of the HVG graph shown in Fig. 5(b), the CI for the maximum node degree with coupling strength at $\varepsilon = 1.2$ always stays at zero while the CIs with coupling strengths $\varepsilon = 2.2$ and $\varepsilon = 2.8$ increase in steps with the increase of data length. The CI for coupling strength $\varepsilon = 2.2$ reaches to a stable value $C_{km} = 100\%$ at data length $N_T = 22$ while the CI for coupling strength $\varepsilon = 2.8$ does not reach to a constant for the largest presented data length. It is worth noting that the key issue for pre-warning catastrophe is to distinguish the difference between the stable state (single period motion) and the transition state (multi-harmonic motions) using sensitivity index CI. In comparison with the two approaches we can see that using the HVG can have more obvious discriminability than that of the VG method, and the change rate of CI for the HVG method about the transition state is much larger than that of the VG method with same data length. The necessary data length for HVG method $(N_T > 1)$ is shorter than that for the VG method $(N_T > 6)$ in terms of the discrepancy between stable state (black line) and the transition state (red line).

Similarly to Fig. 5, Fig. 6 illustrates the CI for the average node degree of the VG method and the CI for the maximum node degree of the HVG method under the change of sampling frequency for three different coupling strengths. In order to get rid of the influence of data length on the analysis of sampling frequency, we take the sufficient data length $N_T = 50$ (see Fig. 5). From Fig. 6(a) we can see that the CI for the average node degree with coupling strength $\varepsilon = 1.2$ for a stable state always stays at zero. The CI for the average node degree with coupling strength $\varepsilon = 2.2$ and $\varepsilon = 2.8$ have dramatic changes for small sampling frequency $f < 15$, and then tend to stable values with $C_{\langle k\rangle} = 10\%$ for coupling strength $\varepsilon = 2.2$ and $C_{\langle k\rangle} = 20\%$ for coupling strength $\varepsilon = 2.8$. From Fig. 6(b) we can see that the CI for the maximum node degree of the HVG graph with coupling strength $\varepsilon = 1.2$ for a stable state always stays zero. The CI for the maximum node degree with coupling strength $\varepsilon = 2.2$ and $\varepsilon = 2.8$ are fluctuated around a certain constant value and there are small discriminations between the transition and the large oscillation state while there are obvious discriminations between the AD state and the transition state. In comparison with the two approaches, we can see that the change rate of the CI of the HVG method between the stable state and the transition state is more obvious than that of the VG algorithm for the same sampling frequency.

For a real system, the catastrophe is commonly induced by the time varying parameter. In what following, a simple example that the wave height changes with time is considered, shown in Fig. 7. In a monitoring process, the index CI needs to be updated constantly from feeding data. For every sampling time to obtain a new data point (node), we drop the first data point (node) of the original network to guarantee the same pre-set data length, and then reconstructing a new network and calculating the topological characteristic to update CI. We consider the case that the wave height is a constant $a = 1$ m in the beginning and gradually increases after time $t = 1500$ s until the height reaches to $a = 2.5$ m at time $t = 3500$ s, show in Fig. 7(a). The corresponding response time series for state variable z_3 is shown in Fig. 7(b). From Fig. 7(b) we can see that the response is initially a weak oscillation state with single harmonic motion even if the amplitude increases due to the increased wave amplitude. The amplitude is magnified in a rapid fashion at a critical value of $t = 4415$ s which indicates the onset of engineering disaster. The CI for the average node degree of the VG method and the CI for the maximum node degree of the HVG method mapped from corresponding time series is illustrated in Fig. 7(c) and (d). From Fig. 7(c) we can see that the CI for the average node degree is not a strict constant value but has a very weak fluctuation around zero even in the stable region of the floating system and the fluctuation amplitude of the CI for the average node degree is about $C_{\langle k\rangle} = 2\%$. When we reexamine the CI for the average node degree of weak oscillation state, we find that the fluctuation period coincides with the period of response because of the boundary effect of the data. For the change rate of the CI in the region just before the catastrophe (shown in the partial enlarged drawing in Fig. 7(c)), we can see that there is

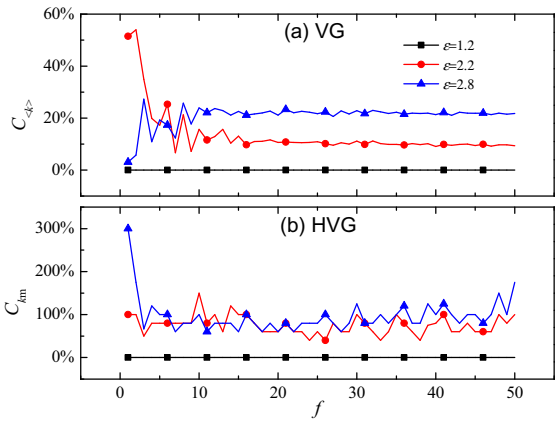

Fig. 6. (a) The CI for the average node degree of the visibility graph theory and (b) the CI for the maximum node degree of the horizontal visibility graph theory as a function of sampling frequency for the data length $N_T = 50$.

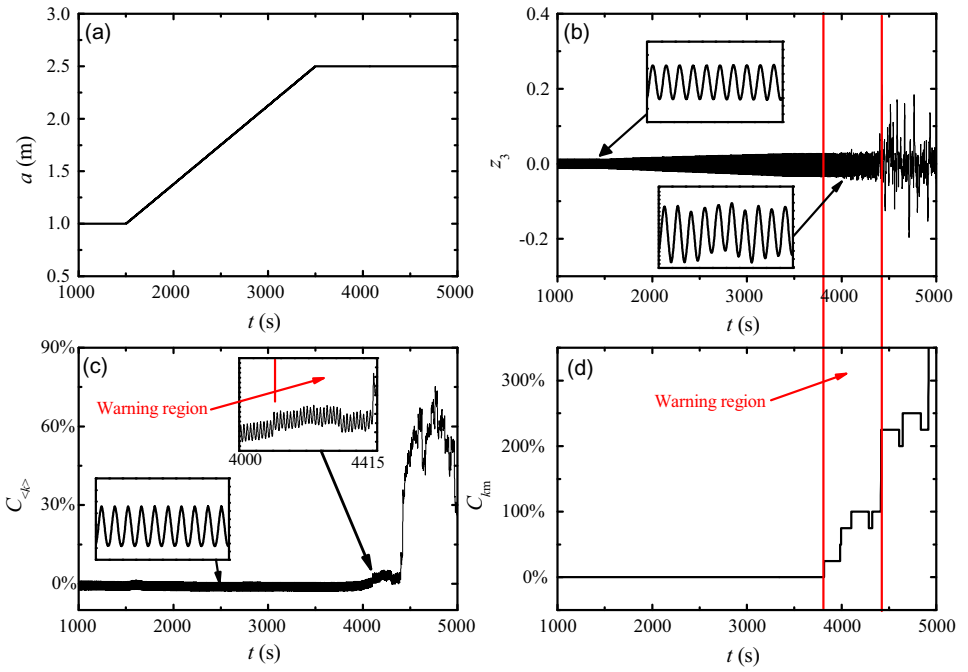

Fig. 7. The variation of (a) the wave amplitude, (b) the corresponding response amplitude operator of the state variable z_3 and (c) the CI for the average node degree of the visibility graph theory, (d) the CI for the maximum node degree of the horizontal visibility graph theory with for sampling frequency $f = 100$ and data length $N_T = 20$.

a weak jumping for the CI at the time $t = 4250$ s and the index CI still has fluctuation after the jumping. With the increase of time, the fluctuation of CI in the region before the catastrophe is disordered in comparison with the CI in the stable region. Thus the region of 4250 s $\leqslant t <$ 4415 s is defined as the pre-warning region for the VG method. For the HVG method, the sensitive index CI for the maximum node degree is shown in Fig. 7(d). From Fig. 7(d) we can see that the CI for the maximum node degree stays at zero for the stable region of the floating system even if the response amplitude increases due to the increased wave amplitude. With the increase of time, the CI for maximum node degree has an obviously stepped increasing at the time $t = 3814$ s prior to the happening of catastrophe, which provides a pre-warning for the oncoming catastrophe. Close to the occurrence of catastrophe, the CI for the maximum node degree reaches to $C_{km} = 100\%$. In comparison with the two methods discussed above, the variation of the pre-warning index C_{km} for the HVG method is more sensitive than that of the pre-warning index $C_{\langle k\rangle}$ for the VG method. Meanwhile, the pre-warning time for the HVG ($T_{HVG} = 601$ s) shown in Fig. 7(d) is also longer than that for the VG method ($T_{VG} = 165$ s) shown in Fig. 7(c). Thus the HVG is superior to the VG method in terms of a pre-warning scheme.

According to above numerical simulations and results analysis, we can conclude that the technical route, using complex network theory to predict catastrophes, is feasible. Nevertheless, we would like to remark that the numerical simulations demonstrate a promising potential of this method and the actual performance needs to be experimentally tested, which has been scheduled in our future work. In addition, for the timeliness of the prediction process, we can use the fast algorithm proposed in the Ref. [43] to construct the VG or HVG graph and the computational complexity of constructing a graph is $O(n)$ for a graph with n nodes. In order to alert us that the catastrophe is going to happen for a realistic application, we should first determinate a critical value regarded as a prediction value.

4. Conclusions

In this paper, we first propose to use the complex network theory to predict potential catastrophes of the complex system. The feasibility of the method is illustrated according to the numerical simulation using visibility graph theory to predict catastrophes of a non-autonomous network which derived from a marine system. Numerical results show that there is an obvious corresponding relationship between the topology characteristics of the networks and the onset of catastrophes. The average degree or maximum degree, of the network graphs constructed from time series with visibility graph or horizontal visibility algorithm, will increase when the catastrophe is going to happen. The Catastrophe Index (CI) as a numerical indicator to measure a qualitative change from a stable state to a catastrophic state is proposed. The two approaches, from visibility graph or horizontal visibility theory, are compared using CI via analyzing the reliability with different data lengths and sampling frequencies. At last, an example for the predicting problem considering time varying parameter is illustrated. It

is worth to notice that using the technique of the virtual network to predict potential catastrophes is not restricting to the particular floating system, which can potentially extendable to catastrophe prediction of other engineering systems or fault detection and diagnosis of mechanical system [44].

Acknowledgements

This work was supported by the National Natural Science Foundation of China [grant numbers 11702088, 11472100]; and the High-tech Ship Research Projects Sponsored by MIIT.

References

[1] J.D. Coval, J.W. Jurek, E. Stafford, Economic catastrophe bonds, Am. Econ. Rev. 628–666 (2009).
[2] C. Loehle, Catastrophe theory in ecology: a critical review and an example of the butterfly catastrophe, Ecol. Modell. 49 (1989) 125–152.
[3] R.F. Mould, Chernobyl Record: the Definitive History of the Chernobyl Catastrophe, CRC Press, 2000.
[4] D. Bourc'his, T.H. Bestor, Meiotic catastrophe and retrotransposon reactivation in male germ cells lacking Dnmt3L, Nature 431 (2004) 96–99.
[5] M. Kurant, P. Thiran, Layered complex networks, Phys. Rev. Lett. 96 (2006) 138701.
[6] S. Panzieri, R. Setola, Failures propagation in critical interdependent infrastructures, Int. J. Model. Identif. Control. 3 (2008) 69.
[7] F.E.M. WEF, Global Risks 2013, in: World Economic Forum, 2013.
[8] D. Helbing, Globally networked risks and how to respond, Nature 497 (2013) 51–59.
[9] S.V. Buldyrev, R. Parshani, G. Paul, H.E. Stanley, S. Havlin, Catastrophic cascade of failures in interdependent networks, Nature 464 (2010) 1025–1028.
[10] W.X. Wang, R. Yang, Y.C. Lai, V. Kovanis, C. Grebogi, Predicting catastrophes in nonlinear dynamical systems by compressive sensing, Phys. Rev. Lett. 106 (2011) 154101.
[11] T. Poston, I. Stewart, Catastrophe Theory and its Applications, Courier Corporation, 2014.
[12] A. Wilson, Catastrophe Theory and Bifurcation: Applications to Urban and Regional Systems, Routledge, 2011.
[13] O. Nelles, Nonlinear System Identification: From Classical Approaches to Neural Networks and Fuzzy Models, Springer Science & Business Media, 2013.
[14] J.D. Farmer, J.J. Sidorowich, Predicting chaotic time series, Phys. Rev. Lett. 59 (1987) 845–848.
[15] M.B. Kennel, R. Brown, H.D.I. Abarbanel, Determining embedding dimension for phase-space reconstruction using a geometrical construction, Phys. Rev. A 45 (1992) 3403–3411.
[16] F. Takens, Detecting Strange Attractors in Turbulence, Springer, 1981.
[17] D.J. Watts, S.H. Strogatz, Collective dynamics of "small-world" networks, Nature 393 (1998) 440–442.
[18] A.-L. Barabási, Scale-free networks: a decade and beyond, Science 325 (2009) 412.
[19] M. Newman, Networks: An Introduction, OUP Oxford, 2010.
[20] J.F. Donges, Y. Zou, N. Marwan, J. Kurths, Complex networks in climate dynamics, Eur. Phys. J. Spec. Top. 174 (2009) 157–179.
[21] P. Gai, S. Kapadia, Contagion in financial networks, Proc. R. Soc. A Math. Phys. Eng. Sci. 466 (2010) 2401–2423.
[22] R. Milo, S. Shen-Orr, S. Itzkovitz, N. Kashtan, D. Chklovskii, U. Alon, Network motifs: simple building blocks of complex networks, Science 298 (2002) 824–827.
[23] R. Pastor-Satorras, A. Vespignani, Epidemic dynamics and endemic states in complex networks, Phys. Rev. E 63 (2001) 66117.
[24] J. Goldenberg, B. Libai, E. Muller, Talk of the network: a complex systems look at the underlying process of word-of-mouth, Mark. Lett. 12 (2001) 211–223.
[25] J. Zhang, M. Small, Complex network from pseudoperiodic time series: topology versus dynamics, Phys. Rev. Lett. 96 (2006) 238701.
[26] L. Lacasa, B. Luque, F. Ballesteros, J. Luque, J.C. Nuno, From time series to complex networks: the visibility graph, Proc. Natl. Acad. Sci. 105 (2008) 4972–4975.
[27] B. Luque, L. Lacasa, F. Ballesteros, J. Luque, Horizontal visibility graphs: exact results for random time series, Phys. Rev. E 80 (2009) 46103.
[28] A.M. Nuñez, B. Luque, J.P. Gomez, L. Lacasa, Visibility Algorithms: A Short Review, INTECH Open Access Publisher, 2012.
[29] L. Lacasa, R. Flanagan, Irreversibility of financial time series: a graph-theoretical approach, arXiv Prepr. arXiv1601.01980. (2016).
[30] C. Liu, W.-X. Zhou, W.-K. Yuan, Statistical properties of visibility graph of energy dissipation rates in three-dimensional fully developed turbulence, Phys. A Stat. Mech. Its Appl. 389 (2010) 2675–2681.
[31] J.B. Elsner, T.H. Jagger, E.A. Fogarty, Visibility network of United States hurricanes, Geophys. Res. Lett. 36 (2009).
[32] B. Luque, L. Lacasa, F.J. Ballesteros, A. Robledo, Analytical properties of horizontal visibility graphs in the Feigenbaum scenario, Chaos An Interdiscip. J. Nonlinear Sci. 22 (2012) 13109.
[33] X. Li, Z. Dong, Detection and prediction of the onset of human ventricular fibrillation: an approach based on complex network theory, Phys. Rev. E 84 (2011) 62901.
[34] A. Nuñez, L. Lacasa, E. Valero, J.P. Gómez, B. Luque, Detecting series periodicity with horizontal visibility graphs, Int. J. Bifurc. Chaos. 22 (2012) 1250160.
[35] H.C. Zhang, D.L. Xu, C. Lu, E.R. Qi, C. Tian, Y.S. Wu, Connection effect on amplitude death stability of multi-module floating airport, Ocean Eng. 129 (2017) 46–56.
[36] V. Resmi, G. Ambika, R.E. Amritkar, General mechanism for amplitude death in coupled systems, Phys. Rev. E 84 (2011) 46212.
[37] A.-L. Barabási, R. Albert, Emergence of scaling in random networks, Science 286 (1999) 509–512.
[38] D.L. Xu, H.C. Zhang, C. Lu, E.R. Qi, C. Tian, Y.S. Wu, Analytical criterion for amplitude death in nonautonomous systems with piecewise nonlinear coupling, Phys. Rev. E 89 (2014) 42906.
[39] H.C. Zhang, D.L. Xu, C. Lu, S.Y. Xia, E.R. Qi, J.J. Hu, et al, Network dynamic stability of floating airport based on amplitude death, Ocean Eng. 104 (2015) 129–139.
[40] H.C. Zhang, D.L. Xu, S.Y. Xia, C. Lu, E.R. Qi, C. Tian, et al, Nonlinear network modeling of multi-module floating structures with arbitrary flexible connections, J. Fluids Struct. 59 (2015) 270–284.
[41] H.C. Zhang, D.L. Xu, C. Lu, E.R. Qi, J.J. Hu, Y.S. Wu, Amplitude death of a multi-module floating airport, Nonlinear Dyn. 79 (2015) 2385–2394.
[42] The Open Graph Viz Platform. <https://gephi.org/>.
[43] G. Zhu, Y. Li, P.P. Wen, An efficient visibility graph similarity algorithm and its application on sleep stages classification, in: F.M. Zanzotto, S. Tsumoto, N. Taatgen, Y. Yao (Eds.), Brain Informatics, Springer, Berlin Heidelberg, 2012, pp. 185–195.
[44] M. Zhang, Z. Jiang, K. Feng, Research on variational mode decomposition in rolling bearings fault diagnosis of the multistage centrifugal pump, Mech. Syst. Signal Process. 93 (2017) 460–493.